# Data-Driven Models for Sub-Cycle Dynamic Response of Inverter-Based Resources Using WMU Measurements

Fatemeh Ahmadi-Gorjayi, Student Member, IEEE, Hamed Mohsenian-Rad, Fellow, IEEE

Abstract—Using real-world data from Waveform Measurement Units (WMUs), this paper proposes novel data-driven methods to model the dynamic response of inverter-based resource (IBR) to the high-frequency disturbances that occur in practice in power systems. WMUs are an emerging class of smart grid sensors. They can capture the fast sub-cycle dynamics in power systems, which are overlooked by phasor measurement units (PMUs). After extracting the differential voltage and current waveforms from the raw waveform data, we develop multiple methods that include data-driven model library construction and proper model selection. One class of methods is proposed in frequency domain, which is based on modal analysis. Another class of methods is proposed in time domain, which is based on regression analysis of time-series. Experimental results based on real-world WMU data demonstrate the of performance the proposed methods.

*Keywords*— Inverter-based resources, data-driven, dynamic response, WMU, modal analysis, regression, disturbance, waveform measurements, synchro-waveform measurements, solar inverters.

#### I. Introduction

With the increasing penetration of inverter-based resources (IBRs), power systems are becoming more complex and more dynamic. Further, the recent incidents with the unexpected responses of IBRs to system-wide disturbances, such as in California, have underlined the need to monitor and characterize the dynamic behavior of IBRs at *high-resolution waveform levels*, such as within the short period of one AC cycle [1].

However, the measurements from phasor measurement units (PMUs) that are commonly used in this field do *not* provide the type of data that is needed for this kind of analysis.

Instead, we need to use the measurements from waveform measurement units (WMUs). WMUs are a new class of smart grid sensors that have emerged only recently [2, Section 4.6]. WMUs provide time stamped waveform measurements.

In this paper, we use WMU data from a pilot project in California to address the above open problem. Specifically, we develop new *data-driven* methods to estimate the dynamic response of IBRs to system-wide sub-cycle disturbances.

To the best of our knowledge, this is the first study of its kind. In fact, as it is recently surveyed in [3], the existing methods in this field can be divided into two categories. First, there are methods that use the internal physics of the IBR. Clearly, such methods require access to the internal physical systems for each IBR. Second, there are methods that are data-driven. However, so far, the focus has been primarily on using data from PMUs. In this paper we rather use data from WMUs.

# II. PROBLEM STATEMENT

Fig. 1 shows the *real-world* waveform measurements during a system-wide disturbance that is captured by a WMU at a

The authors are with the University of California, Riverside, CA, USA. E-mails: fahma012@ucr.edu and hamed@ece.edu. The corresponding author is H. Mohsenian-Rad. This work is supported in part by CEC grant EPC-16-077 and the NSF INTERN supplement grant 1711944.

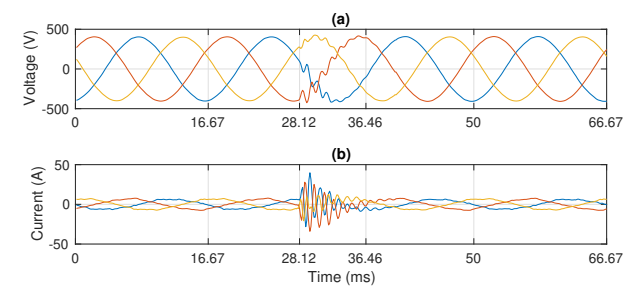


Fig. 1. An IBR's response to a real-world system-wide sub-cycle disturbance: (a) the disturbance causes momentary distortions in voltage waveforms; (b) the dynamic response by the IBR is in form of momentary agitations in current.

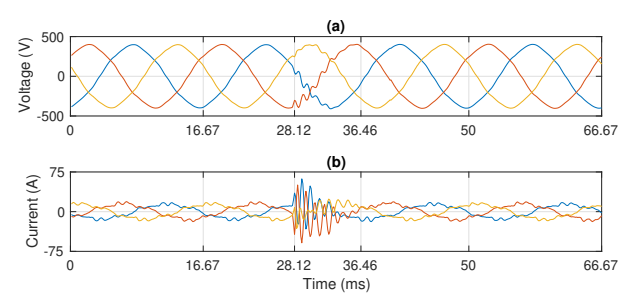


Fig. 2. Another IBR's response to the exact same real-world system-wide sub-cycle disturbance: (a) the voltage distortion at the second IBR; (b) the dynamic response of the second IBR in form of momentary agitation in current.

three-phase PV unit. The disturbance causes a voltage event at the location of the PV inverter. This in turn, causes an agitation (response) in the PV inverter's current waveforms.

The impact of the *exact same disturbance* on another PV unit is shown in Fig. 2. The measurements in this figure are from another WMU. They are time-synchronized with the measurements at the first WMU. Thus, the measurements in Figs. 1 and 2 provide us with *synchro-waveform measurements*, to enable us compare the dynamic response of the two PV inverters (i.e., the two IBRs) to the same disturbance; see [4]. Importantly, the second IBR is located on a different feeder. Notice that, the response of the IBR in Fig. 2(b) is different from the response of the IBR in Fig. 1(b). Whether in Fig. 1 or in Fig. 2, the disturbances as well as the responses of the IBRs are all very short, lasting only about half of a cycle.

# A. IBR as a Dynamic System at Waveform Level

Based on the above examples, each IBR can be seen as a dynamic system that responds to the very fast and very short disturbances in the power system. Each IBR responds to the disturbances based on its own unique internal dynamics.

Accordingly, we can model the behavior of each IBR at waveform level as a dynamic system. Such dynamic system can be represented as an input-output box, as shown in Fig. 3. Here, the input signal is the disturbance in voltage waveform at the terminals of the IBR, and the output signal is the agitation in the IBR's current waveform in response to the disturbance.

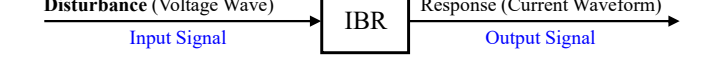




Fig. 3. The waveform-level input-output dynamic model of an IBR.

#### B. Waveform Representation in Differential Form

The disturbance in voltage waveforms as well as the IBR's dynamic response in the current waveforms can be best anlyzed once they are represented in *differential form*. Let time  $t_0$  denote the moment when the disturbance starts. We can express the differential waveform corresponding to waveform x(t) with respect to the event as follows [2, Section 4.2.5]:

$$\Delta x(t) = x(t) - x(t - T), \quad \forall \ t \ge t_0, \tag{1}$$

where T=1/60 seconds is the waveform interval. Time  $t_0$  can be obtained by using the existing methods in [2, Section 4.2]. Fig. 4 shows the differential waveforms corresponding to the disturbance in Fig. 1. Only Phase A is shown here. We can now clearly see the fast dynamic behavior of the IBR at this short interval; which is caused in response to the disturbance.

# C. Our Objective

For the rest of this paper, our objective is to develop *data-driven* models to capture the dynamic response of the IBR, i.e., to predict the IBR's injected current in differential waveform in response to a disturbance in voltage in differential waveform.

# III. MODEL CONSTRUCTION IN FREQUENCY DOMAIN USING MODAL ANALYSIS AND LIBRARY DEVELOPMENT

Consider the differential voltage waveform (input signal) in Fig. 4(a) and the differential current waveform (output signal) in Fig. 4(b). We refer to them as  $\Delta v(t)$  and  $\Delta i(t)$ . By applying the modal analysis, such as the Prony method [2, Section 2.6.3], we can express these two differential waveforms as:

$$\Delta v(t) = \sum_{m=1}^{M} A_m e^{\sigma_m t} \cos(\omega_m t + \phi_m), \qquad (2)$$

$$\Delta i(t) = \sum_{m=1}^{M} B_m e^{\sigma_m t} \cos(\omega_m t + \psi_m), \tag{3}$$

where M denotes the number of dynamic modes. Each dynamic mode m is represented by angular frequency  $\omega_m$  and damping factor  $\sigma_m$ . The differential voltage waveform at mode m is represented by magnitude  $A_m$  and phase angle  $\phi_m$ . The differential current waveform at mode m is represented by magnitude  $B_m$  and phase angle  $\psi_m$ . Accordingly, at each mode m, we can define the equivalent admittance of the IBR at that particular mode as the following complex number:

$$\mathbf{H}_{m} = \frac{B_{m} \angle \psi_{m}}{A_{m} \angle \phi_{m}} = \frac{B_{m}}{A_{m}} \angle (\psi_{m} - \phi_{m}) \quad \text{at} \quad \omega_{m} + j\sigma_{m}. \quad (4)$$

# A. Data-Driven Library Construction

Suppose the voltage and current waveforms are available from a WMU at an IBR during K disturbances. Let  $\Delta v^1(t), \ldots, \Delta v^K(t)$  denote the differential voltage waveforms and  $\Delta i^1(t), \ldots, \Delta i^K(t)$  denote the differential current

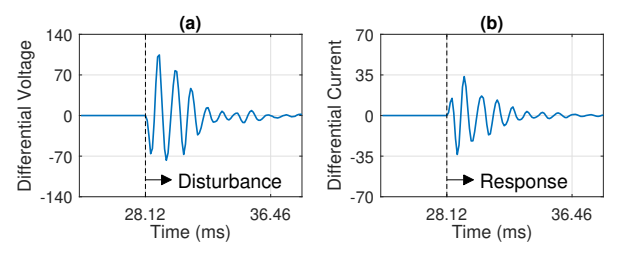


Fig. 4. Differential waveforms for Phase A of the waveforms in Fig. 1.

waveforms during disturbances k = 1, ..., K. By applying the analysis in (2)-(4) to the above measurements, we can obtain:

$$\mathbf{H}_m^k \quad \text{at} \quad z_m^k = \omega_m^k + j\sigma_m^k, \qquad k = 1, \dots, K, \\ m = 1, \dots, M. \tag{5}$$

Each model in (5) corresponds to *one* dynamic mode that is derived from the analysis of *one* disturbance; thus adding up to build a *library* of  $K \times M$  models using modal analysis.

#### B. Data-Driven Model Selection

Let  $\Delta v_{\rm test}(t)$  denote the differential voltage waveform for the given disturbance. Let  $\Delta i_{\rm test}(t)$  denote the differential current waveform for the response of the IBR to this disturbance. Given  $\Delta v_{\rm test}(t)$ , we seek to estimate  $\Delta i_{\rm test}(t)$  based on the model library in (5). We denote our estimate by  $\hat{\Delta i}_{\rm test}(t)$ .

Let us denote the dynamic modes of the test input signal  $\Delta v_{\text{test}}(t)$  by  $z_{n,\text{test}} = \omega_{n,\text{test}} + j\sigma_{n,\text{test}}$ , where  $n = 1, \dots, M$ . For any such dynamic mode n, we define  $k_n^*$  and  $m_n^*$  as follows:

$$[k_n^{\star}, m_n^{\star}] = \underset{k,m}{\operatorname{arg \, min}} \left| z_{n, \text{test}} - z_m^k \right|^2. \tag{6}$$

Here, we select one dynamic mode from the library in (5) that has the *minimum distance* from dynamic mode n of the test input signal. We estimate the IBR's response to  $\Delta v_{\text{test}}(t)$  as:

$$\hat{\Delta i}_{\text{test}}(t) = \sum_{n=1}^{M} C_n e^{\sigma_{n,\text{test}} t} \cos(\omega_{n,\text{test}} t + \varphi_n), \tag{7}$$

where

$$C_n = A_{n,\text{test}} \left| \mathbf{H}_{m_n^{\star}}^{k_n^{\star}} \right|, \quad \varphi_n = \phi_{n,\text{test}} + \angle \mathbf{H}_{m_n^{\star}}^{k_n^{\star}}.$$
 (8)

Here,  $A_{n,\text{test}}$  and  $\phi_{n,\text{test}}$  are the magnitude and phase angle for modal representation of  $\Delta v_{\text{test}}(t)$  at its dynamic mode  $z_{n,\text{test}}$ . We use the magnitude and phase angle of the proper equivalent admittance from the model library to obtain  $C_n$  and  $\phi_n$  in (8), which we use in (7) to estimate the IBR's response, denoted by  $\hat{\Delta}i_{\text{test}}(t)$ . As for indices  $k_n^*$  and  $m_n^*$  that are used in (8), they are defined in (6) and are used in order to select the proper model among the equivalent admittances in the model library. Notice that matrix  $\mathbf{H}$  is defined in (4). In order to select the proper choice of  $\mathbf{H}$  from the library of models in (5), we use indices  $m_n^*$  and  $k_n^*$ , which are defined in (6).

# IV. MODEL CONSTRUCTION IN TIME DOMAIN USING REGRESSION ANALYSIS AND LIBRARY DEVELOPMENT

Again consider the differential waveforms in Fig. 4. In this section, we represent  $\Delta v(t)$  as  $\Delta v[1], \Delta v[2], \ldots, \Delta v[N]$ , which is a discrete time-series, where N is the number of samples. Similarly, we represent  $\Delta i(t)$  as  $\Delta i[1], \Delta i[2], \ldots, \Delta i[N]$ .

# A. Data-Driven Library Construction

Next, we use two different time-domain models, with and without auto-regression, to build the data-driven model library:

1) Approach 1: Using FIR Models: The response of the IBR is constructed by a Finite Impulse Response (FIR) model:

$$\Delta i[\tau] = b_1 \Delta v[\tau] + b_2 \Delta v[\tau - 1] + \dots + b_{n_b} \Delta v[\tau - n_b + 1]. \tag{9}$$

The above FIR model estimates each sample of the output signal as a weighted sum of the  $n_b$  most recent samples of the input signal. Here,  $n_b$  denotes the order of the model.

2) Approach 2: Using ARX Models: The IBR's response is constructed by an Auto-Regressive eXogenous (ARX) model:

$$\Delta i[\tau] = a_1 \Delta i[\tau - 1] + \dots + a_{n_a} \Delta i[\tau - n_a] + b_1 v[\tau] + b_2 \Delta v[\tau - 1] + \dots + b_{n_b} \Delta v[\tau - n_b + 1].$$
 (10)

This ARX model estimates each sample of the output signal as a weighted sum of the  $n_b$  most recent samples of the input signal and the  $n_a$  most recent samples of the output signal itself. Here,  $n_a$  and  $n_b$  denote the order of the model.

Given the K training data sets, we can use (9) or (10) to build a library of K FIR models or K ARX models. For each model, we need to estimate the corresponding unknowns as:

$$\boldsymbol{\theta}_{\text{FIT}} = [b_1, \cdots, b_{n_b}]^\top, \tag{11}$$

$$\boldsymbol{\theta}_{\text{ARX}} = [a_1, \cdots \ a_{n_a}, b_1, \cdots, b_{n_b}]^{\top}. \tag{12}$$

Vectors  $\theta_{FIT}$  and  $\theta_{ARX}$  can be obtained using methods such as Least Square (LS) optimization, e.g., [5, Section 3.2].

# B. Model Selection

Similar to the analysis in Section III-B, we need a method to select the proper model from the library. However, since we do not use modal analysis in Section IV, we select the model based on directly comparing the time series of the test input signal and the time series of the training input signals:

$$k^{\star} = \underset{k}{\operatorname{arg\,min}} \sum_{\tau=1}^{N} \left| v^{k}[\tau] - v_{\text{test}}[\tau] \right|^{2}. \tag{13}$$

Given  $k^*$ , we can estimate  $\Delta i_{\text{test}}(t)$  by using either the FIR model in (9) and (11) or the ARX model in (10) and (12).

#### V. POTENTIAL APPLICATIONS

The analysis in this paper can be used in various potential applications. First, the models for the dynamic response of IBRs can be used for *diagnosis* purposes to enhance the life span of IBRs. This can be done by comparing the derived data-driven models with the nominal/reference models that are provided by the IBR manufacturers. Another option is to *regularly monitor* the dynamic behavior of each IBR over time. A major change can potentially indicate an *incipient failure* that may suggest the need for inspection or maintenance. Second, modeling the sub-cycle dynamic behavior of IBRs may also help with developing digital twins for different types of IBRs to predict how different IBRs may respond to various disturbances in power systems. This can ultimately help with identifying the type and magnitude of disturbances that are likely to cause undesirable tripping of IBRs; see [1] for a

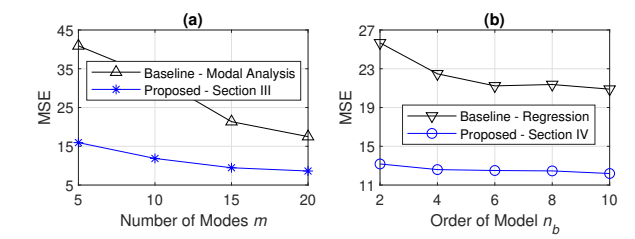


Fig. 5. Performance comparison with the corresponding baseline methods: (a) for the method in Section III; (b) for the method in Section IV.

related discussion. Third, the analysis in this paper can also be used to *compare* the dynamic response of a large group of IBRs in a given geographical region. Such analysis may also shed light on potential *ripple effects* in the power system that may follow a system-wide disturbance due to the agitations in power production or even momentary secession of IBRs.

#### VI. EXPERIMENTAL RESULTS

In this section, we apply the proposed methods to the *real-world* waveform measurements that are obtained by a WMU at a 480 V / 100 kW PV unit, for six months. In total, 63 sub-cycle system-wide disturbances and the corresponding responses of the IBR were recorded in this period. Out of the 63 available disturbances, we used 42 disturbances for training the model, i.e., two third of the available disturbances in the data set is used for training. The remaining 21 disturbances are used for testing the accuracy of the model, i.e., one third of the available disturbances in the data set is used for testing. As a result, we evaluated the *out-of-sample* performance of the proposed models; because the samples that we used for performance evaluation had *no overlap* with the samples that we used to obtain (i.e., train) the models.

1) Comparison with Baseline Methods: As the baseline method to be compared with the design in Section III, we consider a method that applies multi-signal modal analysis to all the 42 training data sets to develop a single model in frequency domain. That is, unlike our proposed method in Section III, this baseline method does not involve the library construction in (5) and the model selection in (6). The results are shown in Fig. 5(a), in terms of the Mean Squared Error (MSE) for each method. As we can see, both methods improve as we increase the number of modes. However, the proposed method always performs much better than the baseline method.

As the baseline method for the design in Section IV, we consider a method that applies multi-signal regression to all the 42 training data sets to develop a *single* model in time domain. That is, *unlike* our proposed method in Section IV, this baseline method does *not* involve library construction and model selection. The results are shown in Fig. 5(b). In both cases, we use FIR models. As we can see, the proposed method always performs much better than the baseline method.

2) Analysis of Modal Distance: For the method in Section III, it is insightful to examine the MSE as a function of the modal distance between each test input signal and the training input signals. For each  $\Delta v_{\text{test}}(t)$ , we obtain:

Modal Distance: 
$$\Phi = \sqrt{\sum_{n=1}^{M} \left| z_{n,\text{test}} - z_{m_n^*}^{k_n^*} \right|^2}.$$
 (14)

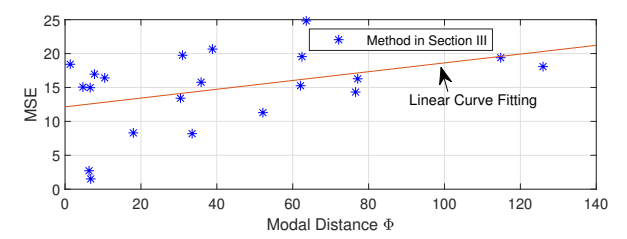


Fig. 6. Plotting the individual MSE of each test case versus the modal distance between the test input signal and the training input signals. Parameter M=6.

TABLE I
MSE FOR USING FIR VS. ARX MODELS IN SECTION IV

	$n_b = 2$	$n_b = 3$	$n_b = 4$	$n_b = 5$
FIR	13.1761	12.7091	12.5947	12.5859
$ARX (n_a = 1)$	12.4331	12.6453	12.4619	12.3848
ARX $(n_a = 2)$	12.5315	12.3748	12.4892	13.4232

The results are shown in Fig. 6. A trend is evident. In general, a higher modal distance for a test input signal leads to a higher MSE in estimating its corresponding test output signal.

3) Using FIR vs. ARX Model: For the proposed method in Section IV, Table I compares the performance of using the FIR model versus the ARX model. The FIR model shows a more stable performance, i.e., its MSE consistently improves as we increase the order of the model. The ARX model rather needs proper tuning of its parameters. However, once such tuning is done, the ARX model can perform slightly better than the FIR model. In fact, the best result in Table I, in bold, is achieved when we use the ARX model with  $n_a = 2$  and  $n_b = 3$ .

# VII. CONCLUSIONS

New data-driven methods were developed and tested to model the dynamic behavior of IBRs when they respond to system-wide sub-cycle waveform disturbances. Experimental results confirmed the high performance of the methods compared to the baselines. They also showed the characteristics of the models, such as in terms of modal distance. This study can provide valuable insights to utilities and independent system operators (ISOs) to enhance their situational awareness and improve stability and reliability of the power system. For example, as mentioned in Section V, modeling the sub-cycle dynamic behavior of IBRs can ultimately help identify the type and magnitude of regional or system-wide disturbances that can cause significant agitation or momentary secession in the power production by IBRs as well as any potential to create ripple effects in the power system.

#### REFERENCES

- A. Silverstein and J. Follum, "High-resolution time-synchronized grid monitoring devices," North American Synchrophasor Initiative Technical Report NASPI-2020-TR-004, Mar. 2020.
- [2] H. Mohsenian-Rad, Smart Grid Sensors: Principles and Applications. Cambridge University Press, UK, Apr. 2022.
- [3] L. Fan, Z. Miao, S. Shah, P. Koralewicz, V.Gevorgian, and J. Fu, "Data-driven dynamic modeling in power systems: A fresh look on inverter-based resource modeling," *IEEE Power & Energy Magazine*, Jun 2022.
- [4] H. Mohsenian-Rad and W. Xu, "Synchro-waveforms: A window to the future of power systems data analytics," *IEEE Power and Energy Magazine (accepted for publication)*, Apr. 2023.
- [5] D. C. Montgomery, C. L. Jennings, and M. Kulahci, Introduction to Time Series Analysis and Forecasting. John Wiley Sons, 2015.

**Fatemeh Ahmadi-Gorjayi** (S'20) received the B.Sc. degree in electrical engineering from Sharif University of Technology, Iran, in 2013, and the M.Sc. degree, Operation Management and Supply Chain (Industrial Engineering) from the University of Tehran, Iran in 2018. She is currently pursuing her Ph.D. degree at the University of California, Riverside, CA, USA. Her research interests include state estimation, power system harmonics, power system planning, and applications of data-driven techniques in power system.

**Hamed Mohsenian-Rad** (M'09-SM'14-F'20) is a Professor of electrical engineering at the University of California, Riverside, CA, USA. His research is on monitoring, data analysis, and optimization of power systems and smart grids. He is the author of *Smart Grid Sensors: Principles and Applications*, Cambridge University Press, 2022. He has served as Editor for the IEEE TRANSACTIONS ON POWER SYSTEMS, IEEE TRANSACTIONS ON SMART GRID and the IEEE POWER ENGINEERING LETTERS.